Published in final edited form as:

Jpn J Ophthalmol. 2009 July ; 53(4): 334–344. doi:10.1007/s10384-009-0687-2.

Noninvasive Functional Imaging of the Retina Reveals Outer Retinal and Hemodynamic Intrinsic Optical Signal Origins

Daniel Ts'o[1], **Jesse Schallek**[1], **Young Kwon**[2], **Randy Kardon**[2,3], **Michael Abramoff**[2,3], and **Peter Soliz**[4]

[1]Department of Neurosurgery, SUNY Upstate Medical University, Syracuse, NY, USA

[2]Department of Ophthalmology and Visual Science, University of Iowa, Iowa City, IA, USA

[3]Veterans Administration, Iowa City, IA, USA

[4]VisionQuest Biomedical, Albuquerque, NM, USA

Abstract

We have adapted intrinsic signal optical imaging of neural activity to the noninvasive functional imaging of the retina. Results to date demonstrate the feasibility and potential of this new method of functional assessment of the retina. In response to visual stimuli, we have imaged reflectance changes in the retina that are robust and spatially colocalized to the sites of stimulation. However, the technique is in its infancy and many questions as to the underlying mechanisms remain. In particular, the source and nature of the activity-dependent intrinsic optical signals in the retina need to be characterized and their anatomic origins determined. The studies described here begin to address these issues. The evidence indicates that the imaged signals are driven by the outer retinal layers and have a dominant hemodynamic component.

Keywords

functional retinal imaging; hemodynamics; intrinsic signals; optical imaging

Introduction

Intrinsic Signal Optical Imaging

Like its counterpart for studies of the neocortex, the retinal imaging technique described here measures functionally correlated reflectance changes in the retina. In the 20 years since its inception and application to studies of the function of mammalian neocortex,[1–3] intrinsic signal optical imaging has become an important tool, widely adopted by neuroscientists. As a technique that provides functional information at the level of cortical columns and areas, it has filled an important gap between electrophysiology at the single-cell level and anatomical and histological methods that reveal structural and compartmental information within cortical areas. Additional key advantages of the technique are its relatively high spatial

Correspondence and reprint requests to: Daniel Ts'o, Department of Neurosurgery, SUNY Upstate Medical University, 750 East Adams Street, Syracuse, NY 13210, USA, dan@tsolab.org.

resolution, its affordability, and its flexibility, including the ease of incorporation into a wide variety of experimental paradigms and stimulus configurations. Indeed, intrinsic signal optical imaging has now been applied in animal studies of nearly every sensory system, often resulting in important new insights into the underlying neurobiology. In addition, the technique has been utilized intraoperatively with appreciable success in the somatosensory, motor, and language areas of human patients.[4–6]

The basis for this technique is the application of modern image acquisition technologies to the measurement of small changes in the optical reflectance of neural tissue due to the modulation of neuronal activity. There are numerous possible biophysical origins for such activity-dependent changes in optical properties, including redox shifts in metabolically important chromophores (e.g., NAD, cytochrome), light scattering due to ionic and/or water movement, and birefringence signals due to membrane conformational changes. The class of optical signals that has received the most attention is related to activity-dependent hemodynamics. These signals dominate in vivo recordings within the spectral band most often utilized, and parallel related signals measured in positron emission tomography (PET) and functional magnetic resonance imaging (fMRI). Within this class, there are two prominent signals: one related to total hemoglobin concentration (which is tied to changes in blood flow and blood volume), and another related to oxygen delivery (the shift between oxy- and deoxyhemoglobin, oximetry). Depending on the recording conditions, these signals in the neocortex are usually quite small, generally in the range of 0.1%–1.0% of total reflectance. It should also be emphasized that, like fMRI and PET, intrinsic signal optical imaging provides only an indirect measure of neuronal activity. The precise nature and mechanism of coupling between neuronal activity and hemodynamics are not completely understood. Nevertheless, even with these uncertainties and the difficulties of recording such small changes, with suitable signal averaging and analysis, careful selection and design of imaging instrumentation, and a stable preparation, it has proven possible, if not routine, to image reliably a wide variety of functional features and patterns of activity in neocortex.

Optical Imaging of the Retina

Even in the early days of our optical imaging work on the visual cortex, we wondered about the feasibility of imaging the function of the retina using a simple modification of the technique. Since one can directly image the retina through the lens of the eye, it was clear that such an approach might have significant potential as a noninvasive method for assessing retinal function not only in experimental animals but also in humans. The technique therefore holds great promise as a tool for both clinical and basic science applications.

Signal Sources and Anatomic Origins

As in the original method of optical imaging in neocortex, the assumption has been that, of the several possible sources of activity-dependent optical signals in the retina, hemodynamics should be at least one contributor. The retina is highly vascularized. The inner retina is fed by the retinal vasculature, while the outer retina is fed by the choroidal circulation. It also has a particularly high rate of oxidative metabolism. Previous studies have demonstrated a change in blood flow and oxygenation in response to visual stimulation.[7,8] The choroidal circulation is known to have a very high flow rate and a small

arteriovenous oxygen saturation difference. In contrast, the retinal circulation nourishing the inner retina, including the ganglion cells, has a much slower flow rate and a high arteriovenous saturation difference.[9]

Other possible signals include activity-dependent light scattering (water or ionic movement, or membrane changes), which should be largely spectrally independent, and shifts in intrinsic chromophores (cytochrome, NAD) or activity-dependent changes in the retinal pigmented epithelium (RPE), each of which will have a characteristic action spectrum. It has been recently discovered that the retina contains a high concentration of neuroglobin, a respiratory protein similar to myoglobin.[10] This finding raises the possibility that neuroglobin may play an important role in the oxygenation of the retina and may contribute to the intrinsic optical signals.

Methods

Construction of the Retinal Functional Imager

To pursue the potential of functional optical imaging in the retina, we have modified a commercially available fundus camera (Topcon Medical Systems, Paramus, NJ, USA) to enable the noninvasive measurement of stimulus-evoked intrinsic optical signals from the retina. A number of considerations prevent the straightforward adaptation of the intrinsic signal optical imaging method to the functional imaging of retina in vivo. Foremost is the obvious fact that the retina is light sensitive in the same spectral band that optical imaging measurements are typically made in the neocortex. To find an appropriate spectral band for imaging of the retina, we chose to make the measurements of intrinsic optical signals outside the visible range, that is, in the near-infrared (NIR) range between 750 and 900 nm (see schematic in Fig. 1). Optical measurements of reflectance changes between 750 and 900 nm do not interfere with visible stimuli between 450 and 650 nm. We presented most stimuli at 540 nm. The illumination source, a tungsten–halogen bulb powered by a stable DC power supply, bounced off a dichroic (hot) mirror designed to reflect only NIR wavelengths, and was also filtered by an NIR interference filter at the chosen illumination wavelength. This NIR illumination light was reflected off an annular mirror and projected forward to illuminate the retina.

Stimuli

A liquid crystal display (LCD) module (Sony, New York, NY, USA) was mounted on the modified fundus camera to project visual stimuli into the retina. This light path was filtered by a green (540 nm) or blue (450 nm) filter before being reflected into the common light path by the dichroic mirror. The stimulus set consisted of either a 40° solid field or a counter-flickering checkered field (8 Hz), or rectangular subsections thereof, including spots and bars of horizontal and vertical orientation at different retinal/spatial locations. Stimulus intensity was typically in the mesopic range (3–8 cd/m^2), except that for the monkey retina, a bright stimulus was often used.

Image Acquisition

Images were typically acquired at a rate of 2 Hz using a 384 × 288 pixel resolution binned 2 × 2. Retinal images in the NIR were collected with a cooled charge-coupled device (CCD) camera (Photometrics, Tucson, AZ, USA), while a visible patterned stimulus generated by a computer-driven LCD was delivered to the retina via a dichroic beamsplitter. A typical single trial consisted of a 2-s (4-frame) prestimulus period, followed by a 3-s (6-frame) stimulus period, followed by a 5-s (10-frame) poststimulus period. Then, an intertrial interval of at least 3 s passed before the next trial began, using a different stimulus randomly picked from the stimulus set. Single recording sessions generally consisted of 8–16 blocks of a set of trials that were exhaustively initiated from a set of stimuli. Image acquisition was synchronized to the electrocardiograph (ECG) and the respiration cycle to permit the reduction of those noise sources from the acquired images. Summary images and signal time courses were viewed online via a color display, and the image data were stored by the host computer.

Image Analysis

Image data were analyzed with either a custom Matlab program (Mathworks, Natick, MA, USA) or other custom programs. Typically, a baseline (prestimulus) differential algorithm was used to extract the changes in retinal reflectance due to a presented stimulus. For each frame, or specific subset (region of interest, ROI), the fractional reflectance change (dR/R) was computed. Typical ROIs used in the analysis were 11 × 11 pixel regions (approximately 1.5°–1.9° field of view).

Electroretinogram

An eye speculum spanning the inferior and superior fornix was used as a transcorneal electrode. Another speculum placed in the unstimulated, unimaged eye served as a reference electrode, and a ground electrode was placed on the stereotaxic frame. Electroretinogram (ERG) signals were passband filtered between 0.5 and 55 Hz and amplified 10 000×. ERG signals were then digitized and acquired with a custom-written Matlab program sampling at 400 Hz. Typically, 60 waveforms were averaged online before data were saved. Stimuli presented yielded long-duration focal ERGs and spanned 35°–45°, rather than Ganzfeld flash ERGs, for two reasons: this approach enabled the use of the same LCD stimulus module and light path to generate the patterned stimuli for the retinal imaging of intrinsic signals as well as to evoke the focal ERGs; and a long-duration luminance step instead of the more traditional Ganzfeld flash permitted the separation of distinct ON and OFF responses of the retina.

Pattern Electroretinogram

The stimulus consisted of a counter-flickering checkerboard pattern with a 40° field of view. Individual check sizes were between 0.4° and 3.2°. The temporal frequency was at a fixed rate of 12 reversals/s. Typically 60–200 pattern electroretinogram (pERG) records were averaged before data were saved for later analysis.

Pharmacological Agents

The drugs were dissolved in a bacteriostatic solution and filtered with a 0.2-um filter. A total volume of 40–80 μl was injected into either the right or the left eye. Final estimated concentrations of 4.8–8.4 μM tetrodotoxin (TTX), 0.83–3.8 mM 2-amino-4-phosphonobutyric acid (APB), and 3.3–3.8 mM cis-2,3-piperidinedicarboxylic acid (PDA) were calculated based on a vitreal volume estimate of 2.1 ml.[11,12] These concentrations are within the range of significant suppression of the ganglion cells and ON and OFF pathways.[12]

Drug Injections

Prior to drug injection, the selected eye was treated with an ophthalmic anesthetic (0.5% proparacaine hydrochloride). A 28–30 gauge needle was inserted posterior to the limbus and angled toward the center of the vitreous humor to ensure proper drug delivery. In the case of the APB+PDA injections, two separate injections were made within minutes of each other in the nasal-superior and temporal–superior angles.

Animal Procedures

Young adult cats (*Felis catus*) and monkeys (*Macaca fascicularis*) were anesthetized with ketamine (10 mg/kg, intramuscular) followed by sodium thiopental (20 mg/kg, intravenous, supplemented by a constant infusion of 1–2 mg/kg per hour). The animals were intubated with an endotracheal tube, paralyzed with vecuronium bromide (0.1 mg/kg per hour), and artificially respirated. The ECG, electroencephalogram, temperature, and expired CO2 were monitored throughout the duration of each experiment. Phenylephrine hydrochloride ophthalmic solution (10%) and atropine (1%) were applied topically to dilate the pupil and inhibit accommodation. The corneas were fitted with low-diopter lenses to inhibit corneal drying. Animals were placed in a stereotaxic frame to provide for a stable recording. Animals were cared for in accordance with the Animal Welfare Act and the U.S. Department of Health and Human Services "Guide for the Care and Use of Laboratory Animals."

Results

Cat Retinal Imaging

Figure 2 displays the imaged responses from the retina of an anesthetized cat to a set of horizontally oriented bars composed of a single row of counter-flickering checks, 2° in width. The retinal field of view was approximately 40°. All images are OD, except when noted otherwise; the optic disc is positioned at the lower right corner of the frame; and the area centralis is roughly at the center of the frame. Typically, the signal is negative (darkening, reflectance decrease) with a peak amplitude in the range of 0.1%–1.0%, expressed as the fractional change in reflectance (dR/R). Both the sign and amplitude of these signals are similar to those found in the neocortex. This series (Fig. 2) demonstrates the remarkable spatial specificity of the recorded retinal response, and the ability to systematically stimulate and target the recordings to specific sites over a large region of the retina.

The negative response (decrease in reflected light) is the reverse of the stimulus contrast, proof that the imaged response is not due to a leak of the stimulus. In addition, the slow rise and fall time course matches intrinsic signals from other neural tissue, and not the sharp onsets and offsets of the stimulus period. The spatial distribution of the recorded retinal response is tightly correlated with the stimulus presented. When a series of checkerboard stimuli of increasing extents was presented, they elicited the expected corresponding increase in the area of activation (not shown).

Figure 3 provides further information about the magnitude and time course of these retinal functional signals, in this case, in response to a focal spot stimulus. Also clearly depicted in this figure is the observation that two distinct signals were often observed, a negative signal that coincided with the spatial location of the presented stimulus, and an adjacent positive signal. The origins and mechanisms underlying this second, positive signal are unknown. Its time course and amplitude are similar to those of the negative signal, but it was not always present even when the negative signal was observed. Most interestingly, it was spatially asymmetric, and generally appeared at the superior–nasal side of the negative signal regardless of which eye was imaged. In this particular example, the signal amplitudes peaked approximately at a dR/R of 1.0%. The signals peaked at 3 s with a decay time of 7–10 s.

In another series of experiments (not shown), the relationship between stimulus duration and response magnitude was studied. Stimulus durations from 200 ms to 30 s were investigated, and an approximately linear relationship with longer stimulus durations resulting in greater response magnitudes was discovered, within the range tested.

In Fig. 4, the "line spread" of the imaged response to a spot (small square) stimulus is demonstrated. The line profile at the bottom, plotted as the signal amplitude at each pixel location across a horizontal slice through the middle of the imaged response, indicates that the line spread in this case was approximately 150 μm across the retina. Particularly striking in this case is how well the square and its corners are reproduced in the spatial pattern of the imaged retinal response.

Except as noted, our experiments used a green visual stimulus (540 nm), and a full study on the dependency of the retinal signals to the wavelength of the stimulus has not been done. However, here an imaging experiment using stimuli in the blue band (450 nm) was conducted to test for a possible contribution of rod activation to these signals. Two different stimulus wavelengths were tested, a 545-nm green close to the standard green that has been used thus far, but missing energy in and around 500 nm, and a blue, also missing 500 nm, peaking at around 450 nm. The 500-nm band was cut out on purpose to make it easier to interpret the results. In particular, the midspectral cones should have a relatively poor responsivity to the 450-nm blue stimulus, whereas the rods should be strongly activated by the blue stimuli. The green and blue stimuli were adjusted for approximately equal radiance, and both stimuli were in the mesopic range. The results demonstrate a marked imaged retinal response to the blue stimulus of a magnitude at least equal to that observed with the green stimulus. Thus, it is likely that the rods provide a significant contribution to our observed signals.

Anatomic Origins

Several different experiments were conducted to determine the anatomic origins and retinal layers driving these functional intrinsic signals. The dependency of the signal amplitude on the spatial frequency of the stimulus pattern was tested to probe the contribution of ganglion cell activity to the imaged signals. In its simplest form, shown in Fig. 5, the imaged retinal response resulting from a static solid (green) bar was compared to the counter-flickering checkered bar used in earlier experiments. As seen in Fig. 5, the solid green bar elicited a greater response than the checkered, counter-flickering bar. Further experiments showed that this increase in response is proportional to the increase in the time-averaged luminance of the solid bar in comparison to the checkered bar. A more complete study over several octaves of spatial and temporal frequency has shown no appreciable tuning of these signals, and signal amplitudes are proportional to the time-averaged luminance. These results indicate that neither cells with a center-surround receptive field nor those with appreciable spatial or temporal frequency tuning are likely the dominant driving activity underlying the imaged signals. Thus, the ganglion cell layer, known to contain cells with center-surround receptive fields, is probably not a major contributor to these observed signals.

Pharmacologic Dissection

A second set of experiments further exploring the anatomic origins of these signals employed pharmacologic dissection of the retinal circuitry through selective inactivation. In the first of these studies, intravitreal injections of the sodium channel blocker tetrodotoxin (TTX) were made to suppress the action potentials in the retina—primarily the ganglion cell layer. The retinal responses to visual patterned stimuli before and after such injections were imaged continuously for several hours. Two independent assays for the effectiveness of the TTX injections were also applied: the pERG was recorded, which allowed monitoring of the decay of the ganglion cell responses over about an hour postinjection, and the abolition of the consensual pupillary light reflex in the uninjected eye was observed when a bright light was presented to the injected eye. Both tests confirmed the effectiveness of the ganglion cell blockage within 2 h after the intravitreal injection of TTX. However, as can been seen in Fig. 6, post-TTX imaging of the retinal response to visual stimuli demonstrated no change in the response magnitude, spatial correlation, or time course of the imaged response, up to 8 h post-TTX. The signals persisted at the same magnitude long after the pERG, and the consensual pupil reflex confirmed the effectiveness of the blockade. These results further support the notion that the dominant retinal layers driving the observed imaged signals are unlikely to include the ganglion cell layer.

An additional set of pharmacologic dissection experiments used APB and PDA to block the ON and OFF bipolar/photoreceptor synapses.[13,14] The experiments were conducted in a manner parallel to the TTX experiments, including the confirmation of the effectiveness of the injections through the monitoring of the pERG, which showed the dropout of the bipolar and ganglion cell contributions, and the abolition of the consensual pupillary reflex. The results of the APB and PDA experiments, seen in Fig. 6, also demonstrated no observable change in the imaged retinal response to presented stimuli, even hours after the drug injection. These results, in combination with the studies showing lack of spatial and temporal frequency tuning, with retinal responses most closely tracking a time-averaged

luminance of the presented stimuli, indicate an outer retinal anatomic origin of the observed signals.

Glaucomatous Cats

Retinal imagings were made in cats, obtained from Dr. Gillian McLellan, that exhibited congenital open-angle glaucoma. Optical coherence tomography (OCT) and pERG studies conducted on these cats demonstrated a marked thinning of the nerve fiber layer and a near absence of the ganglion cell components in the pERG, along with the expected high intraocular pressure. Retinal imaging experiments on these cats showed robust signals with a time course matching that of the normal population. These results further confirm the notion that the dominant origin of the retinal signals is probably not the ganglion cells.

Hemodynamics

Apart from the question of what specific form of retinal activity drives these functional signals is the issue of the underlying biophysical mechanism for the observed change in reflectance. Although, based on the pioneering work on the neocortex,[2] it was assumed from early on that at least one of the biophysical origins of the retinal signals might be attributed to hemodynamic sources, yet this notion still remains to be proven. In previous studies, particularly in neocortex, one type of evidence used to support the notion of a hemodynamic component in the recorded signals has been the characteristics of the signal dependence on the wavelength of illumination. Such experiments were conducted here in the retina, and the results demonstrate that, using illumination wavelengths between 700 and 900 nm, the signal amplitude diminishes monotonically with the increase in wavelength. For example, the signal size at 855 nm was roughly one-fifth of that at 750 nm, which roughly corresponds to the drop in hemoglobin absorption between these wavelengths. This behavior in wavelength dependency does not match that expected due to oximetry (i.e., oxy/deoxyhemoglobin absorption ratio) alone. Since the wavelength dependency is monotonically decremental between 700 and 900 nm, there is no reversal at the isosbestic point of oxy/deoxyhemoglobin at 805 nm. These results suggest that the biophysical mechanism of the observed functional reflectance change is unlikely to be dominated by oximetry, and that either changes in total hemoglobin or blood volume may be a candidate.

Additional retinal imaging experiments using systemic injections of blood contrast agents were conducted to further explore the possible role of hemodynamics in the generation of the observed signals. The first agent was nigrosin, a dark dye ("India ink") with a strong, broad absorption profile in the visible range but a monotonically diminishing absorption rate in the near infrared. Retinal imaging was conducted both before and after the nigrosin injection. In the first observation the total retinal reflectance dropped dramatically immediately after the dye injection. Figure 7 shows the results of functional retinal imaging in response to a visual stimulus both before and after the dye injection. As can be seen, the change in reflectance due to the visual stimulus (dR/R) doubled after the nigrosin injection, as compared with the preinjection measurements. These results are consistent with a signal source mechanism linked to a change in total blood volume. A second set of blood contrast agent experiments (not shown) used indocyanine green (ICG) dye. The primary advantage of ICG in this context is that its absorption spectrum is markedly different from that of

hemoglobin, having a peak at around 800 nm. When compared to wavelength dependency measurements of the retinal functional signals taken prior to a systemic injection of ICG, the wavelength dependency of these signals after the ICG injection showed a shift in the spectral function mirroring the spectral absorption function of ICG. Taken together, these retinal imaging experiments using blood contrast agents indicate that a dominant component of the observed functional retinal signals is due to a change in blood volume.

The nature of the mysterious, asymmetric positive signal that is clearly seen in Fig. 3 has been of particular interest. This positive signal is not always observed, but when recorded, its time course matches that of the negative signal, providing one piece of evidence that the two signals are possibly linked in their underlying biophysical mechanism. The superionasal asymmetry that the positive signal almost invariably exhibits is in the direction of the path of the incoming retinal circulation, which originates from the optic disc and arcs both superiorly and inferiorly as it fans out temporally. Thus, one of our early hypotheses as to the origin of an asymmetric positive signal was the incoming reoxygenated blood (positive in sign) following the path of the retinal circulation. This explanation may still be viable although there is some newer evidence that is not supportive of this explanation: in this study, preliminary evidence indicated that even when the stimulation was moved further in a nasal direction, the asymmetry never reversed along the temporal–nasal axis. A related hypothesis for the origins of the positive signal is that it reflects some form of "blood stealing" by the activated retina from the adjacent retina. An analogous observation of blood stealing in the brain has been reported in fMRI studies.[15,16]

In the present experiments, one of the observations made to further investigate the nature of this positive signal was a study of the possibility of inverting the signs of both the negative and positive signals with reverse contrast stimuli. One such experiment is depicted in Fig. 8, in which the same cat retina was presented with a standard, positive (bright) stimulus contrast (a green solid bar on a black background), and then an inverted contrast stimulus (a dark bar on a green background). The positive contrast stimulus evoked the standard negative signal response at the stimulated retinal site and a nasally adjacent positive signal response. The inverted stimulus, however, yielded an opposite polarity from each retinal site, a positive signal at the retinal site stimulated with the dark (negative) contrast, and a nasally adjacent negative signal. The mechanisms underlying this behavior are not presently understood.

Primate Retinal Imaging

Naturally, we have been interested in the applicability of this retinal functional imaging method for possible clinical use in humans. Previously published studies describe early work demonstrating this retinal functional imaging technique in awake humans.[17] Performing optical imaging in the retina of the awake human presents many obstacles, including shifts in recording position and related illumination shifts, eye movements, blinks, uncontrolled respiratory and cardiac pulsations, unstable tear film, and subject fatigue. Thus, the transport of this imaging methodology to the anesthetized nonhuman primate is of particular interest. Figure 9 shows a comparison between signals observed in the cat and the macaque monkey. As can be seen, the signals recorded in the monkey are of lower amplitude than those

recorded in the cat despite the much greater intensity of the stimulus; the monkey required a stimulus of approximately 1000 times greater brightness to elicit imageable, robust signals. This apparent species difference is not yet understood, yet it seems unlikely that it is due simply to the function of the tapetum lucida in the cat or to its rod-dominated retina. Nevertheless, the use of brighter stimuli does yield robust signals in the primate retina. Other groups studying the primate retina under similar conditions[18–21] also employed bright stimuli, typically generated by the xenon flash in commercial fundus cameras. In other respects, the signals recorded in the primate retina appear to be similar to those observed in the cat, particularly with respect to the time course and spatial properties.

Discussion

The existence of spatially specific optical signals in response to a variety of pattern visual stimuli has been demonstrated by the application of a modification of the cortical optical imaging technique to the noninvasive functional imaging of the retina. Experiments exploring the anatomic and biophysical origins of these signals have provided evidence indicating that the dominant source of retinal activity underlying these signals arises from the outer retina, and that changes in blood volume are likely to be a major contributing component. Further experiments are being done to help resolve these issues. Analogous signals in the primate retina have also been described, though the visual stimuli required are several orders of magnitude brighter. The results suggest that this method holds promise as a future tool both for the researcher and for the clinician as a noninvasive assessment technique of retinal functions.

In a technical tour de force, it has recently been demonstrated that it is possible to use fMRI to visualize patterns of activity in the retina in vivo.[22] In that study, the retinas of anesthetized cats were visually stimulated while being imaged for BOLD (blood oxygenation level-dependent) contrast signals with a 9.4-T scanner, using 1-mm slices and an in-plane resolution of 468 μm × 468 μm. The results represent an independent confirmation of the validity of the principles used in the present technique of optical imaging of retinal function, namely that there exists activity-dependent hemodynamic signals in the retina that are detectable and topographically localized.

Many questions remain as to the exact anatomic and biophysical mechanisms underlying the observed signals and their links to retinal hemodynamics. One particular question that is yet unresolved is a detailed reconciling of the apparent increases in blood volume induced under light stimulation (driven by outer retinal activity) with earlier studies that demonstrate a reduction in the oxygen utilization by the photoreceptors when presented with light stimuli.

Similarly, the studies described here indicate that the dominant retinal activity driving these intrinsic functional signals arises from the outer retina, either from the photoreceptors or perhaps the RPE. They also point to a primarily hemodynamic biophysical mechanism underlying these signals. It is conventionally accepted that the choroidal circulation is the primary blood supply to the outer retina, and that this system is "oversupplied" and does not modulate in response to activity. Thus, the present results may challenge one of these two established notions and suggest instead that either the choroidal circulation can indeed be

modulated, or, perhaps more likely, activity in the outer retina does directly influence the retinal circulation (even without inner retinal activity). Indeed, there does exist evidence that photoreceptors partially draw oxygen supply derived from the retinal circulation (10%–15%)[8,23] and perhaps then modulate its function.

Beyond a hemodynamic mechanism, it has also been reported that similar stimulus-evoked intrinsic optical signals are found in the blood-free in vitro preparation.[24] These findings parallel studies in blood-free neuronal culture work that show intrinsic optical signals correlated with neural activity.[25] Thus, it is likely that other optical signals, typically buried below hemodynamic signals in the in vivo retinal imaging scenario, exist in the retina.

In summary, we have described:

1. A novel retinal functional imaging technique for recording a stimulus-induced optical signal from the retina that is highly spatially resolved within a broad (40°) field.
2. Evidence from the temporal dynamics and action spectra of recorded signals that are consistent with a hemodynamic origin, and are not a stimulus artifact.
3. A second, positive signal in addition to the negative signal that is ephemeral and spatially asymmetric to the negative signal, exhibiting a superior–nasal bias.
4. Studies using blood contrast agents that show an enhancement of signal strength, further supporting a dominant hemodynamic origin to the imaged signals.
5. Studies showing that the suppression of spiking activity in the inner retina (particularly ganglion cells) via intravitreal TTX injections result in no apparent alteration of the imaged signals, a finding not consistent with a ganglion cell signal origin.
6. Studies examining the dependency of the imaged signals on spatiotemporal properties of the stimulus, with no appreciable tuning to the spatial or temporal frequency content of the stimulus being observed, further supporting an outer retinal origin of the signals.
7. Functional imaging of nonhuman primate retina that demonstrates comparable intrinsic signals in primate retina, but showing significantly lower photometric sensitivity than the cat retina.

As this is a review article, readers may be interested in a more comprehensive description of the material covered, which can be found in papers published elsewhere by the authors and their co-researchers.[26,27]

Acknowledgments

The authors wish to thank Mark Zarella, Hongbin Li, Dorothy Joiner, and Sandra McGillis, who all helped make this work possible. Thanks to Dr. Gillian McLellan of the University of Wisconsin for supplying the glaucomatous

cats, and Dr. Suresh Viswanathan of Indiana University for sharing his OCT and pERG data on these glaucomatous cats.

This work was supported by NIH EY12915, EB002843, the American Health Assistance Foundation, and the Glaucoma Research Foundation.

References

1. Grinvald A, Lieke E, Frostig RD, Gilbert CD, Wiesel TN. Functional architecture of cortex revealed by optical imaging of intrinsic signals. Nature. 1986; 324:361–364. [PubMed: 3785405]
2. Frostig RD, Lieke EE, Ts'o DY, Grinvald A. Cortical functional architecture and local coupling between neuronal activity and the microcirculation revealed by in vivo high-resolution optical imaging of intrinsic signals. Proc Natl Acad Sci U S A. 1990; 87:6082–6086. [PubMed: 2117272]
3. Ts'o DY, Frostig RD, Lieke EE, Grinvald A. Functional organization of primate visual cortex revealed by high resolution optical imaging. Science. 1990; 249:417–420. [PubMed: 2165630]
4. Haglund MM, Ojemann GA, Hochman DW. Optical imaging of epileptiform and functional activity in human cerebral cortex. Nature. 1992; 358:668–671. [PubMed: 1495561]
5. Toga AW, Cannestra AF, Black KL. The temporal/spatial evolution of optical signals in human cortex. Cereb Cortex. 1995; 5:561–565. [PubMed: 8590828]
6. Cannestra AF, Blood AJ, Black KL, Toga AW. The evolution of optical signals in human and rodent cortex. Neuroimage. 1996; 3:202–208. [PubMed: 9345491]
7. Riva CE, Harino S, Shonat RD, Petrig BL. Flicker evoked increase in optic nerve head blood flow in anesthetized cats. Neurosci Lett. 1991; 128:291–296. [PubMed: 1945050]
8. Linsenmeier RA. Effects of light and darkness on oxygen distribution and consumption in the cat retina. J Gen Physiol. 1986; 88:521–542. [PubMed: 3783124]
9. Hogeboom van Buggenum IM, van der Heijde GL, Tangelder GJ, Reichert-Thoen JW. Ocular oxygen measurement. Brit J Ophthalmol. 1996; 80:567–573. [PubMed: 8759272]
10. Schmidt M, Giessl A, Laufs T, Hankeln T, Wolfrum U, Burmester T. How does the eye breathe? Evidence for neuroglobin-mediated oxygen supply in the mammalian retina. J Biol Chem. 2003; 278:1932–1935. [PubMed: 12409290]
11. Hood DC, Frishman LJ, Viswanathan S, Robson JG, Ahmed J. Evidence for a ganglion cell contribution to the primate electroretinogram (ERG): effects of TTX on the multifocal ERG in macaque. Vis Neurosci. 1999; 16:411–416. [PubMed: 10349962]
12. Hare WA, Ton H. Effects of APB, PDA, and TTX on ERG responses recorded using both multifocal and conventional methods in monkey. Doc Ophthalmol. 2002; 105:189–222. [PubMed: 12462444]
13. Slaughter MM, Miller RF. 2-Amino-4-phosphonobutyric acid: a new pharmacological tool for retina research. Science. 1981; 211:182–185. [PubMed: 6255566]
14. Slaughter M, Miller R. An excitatory amino acid antagonist blocks cone input to sign-conserving second-order retinal neurons. Science. 1983; 219:1230–1232. [PubMed: 6131536]
15. Shmuel A, Augath M, Oeltermann A, Logothetis NK. Negative functional MRI response correlates with decreases in neuronal activity in monkey visual area V1. Nat Neurosci. 2006; 9:569–577. [PubMed: 16547508]
16. Shmuel A, Yacoub E, Pfeuffer J, Van de Moortele PF, Adriany G, Hu X, Ugurbil K. Sustained negative BOLD, blood flow and oxygen consumption response and its coupling to the positive response in the human brain. Neuron. 2002; 36:1195–1210. [PubMed: 12495632]
17. Abramoff MD, Kwon YH, Ts'o D, et al. Visual stimulus-induced changes in human near-infrared fundus reflectance. Invest Ophthalmol Vis Sci. 2006; 47:715–721. [PubMed: 16431972]
18. Tsunoda K, Oguchi Y, Hanazono G, Tanifuji M. Mapping cone- and rod-induced retinal responsiveness in macaque retina by optical imaging. Invest Ophthalmol Vis Sci. 2004; 45:3820–3826. [PubMed: 15452094]
19. Nelson DA, Krupsky S, Pollack A, et al. Noninvasive multiparameter functional optical imaging of the eye. Ophthalmic Surg Lasers Imaging. 2005; 36:57–66. [PubMed: 15688972]

20. Hanazono G, Tsunoda K, Shinoda K, Tsubota K, Miyake Y, Tanifuji M. Intrinsic signal imaging in macaque retina reveals different types of flash-induced light reflectance changes of different origins. Invest Ophthalmol Vis Sci. 2007; 48:2903–2912. [PubMed: 17525227]
21. Okawa Y, Fujikado T, Miyoshi T, Hirohara Y, Mihashi T, Tano Y. Contribution of retinal ganglion cell activity to intrinsic signals. Invest Ophthalmol Vis Sci. 2007; 48:3845.
22. Duong TQ, Ngan S-C, Ugurbil K, Kim S-G. Functional magnetic resonance imaging of the retina. Invest Ophthalmol Vis Sci. 2002; 43:1176–1181. [PubMed: 11923263]
23. Birol G, Wang S, Budzynski E, Wangsa-Wirawan ND, Linsenmeier RA. Oxygen distribution and consumption in the macaque retina. Am J Physiol Heart Circ Physiol. 2007; 293:H1696–H1704. [PubMed: 17557923]
24. Yao XC, George JS. Dynamic neuroimaging of retinal light responses using fast intrinsic optical signals. Neuroimage. 2006; 33:898–906. [PubMed: 17000120]
25. Cohen LB. Changes in neuron structure during action potential propagation and synaptic transmission. Physiol Rev. 1973; 53:373–418. [PubMed: 4349816]
26. Schallek JB, Li H, Kardon RH, et al. Stimulus-evoked intrinsic optical signals in the retina: spatial and temporal characteristics. Invest Ophthalmol Vis Sci. 2009 (in press).
27. Schallek JB, Kardon RH, Kwon YH, Abramoff MD, Soliz P, Ts'o D. Stimulus-evoked intrinsic optical signals in the retina: pharmacological dissection reveals outer retinal origins. Invest Ophthalmol Vis Sci. 2009 (in press).

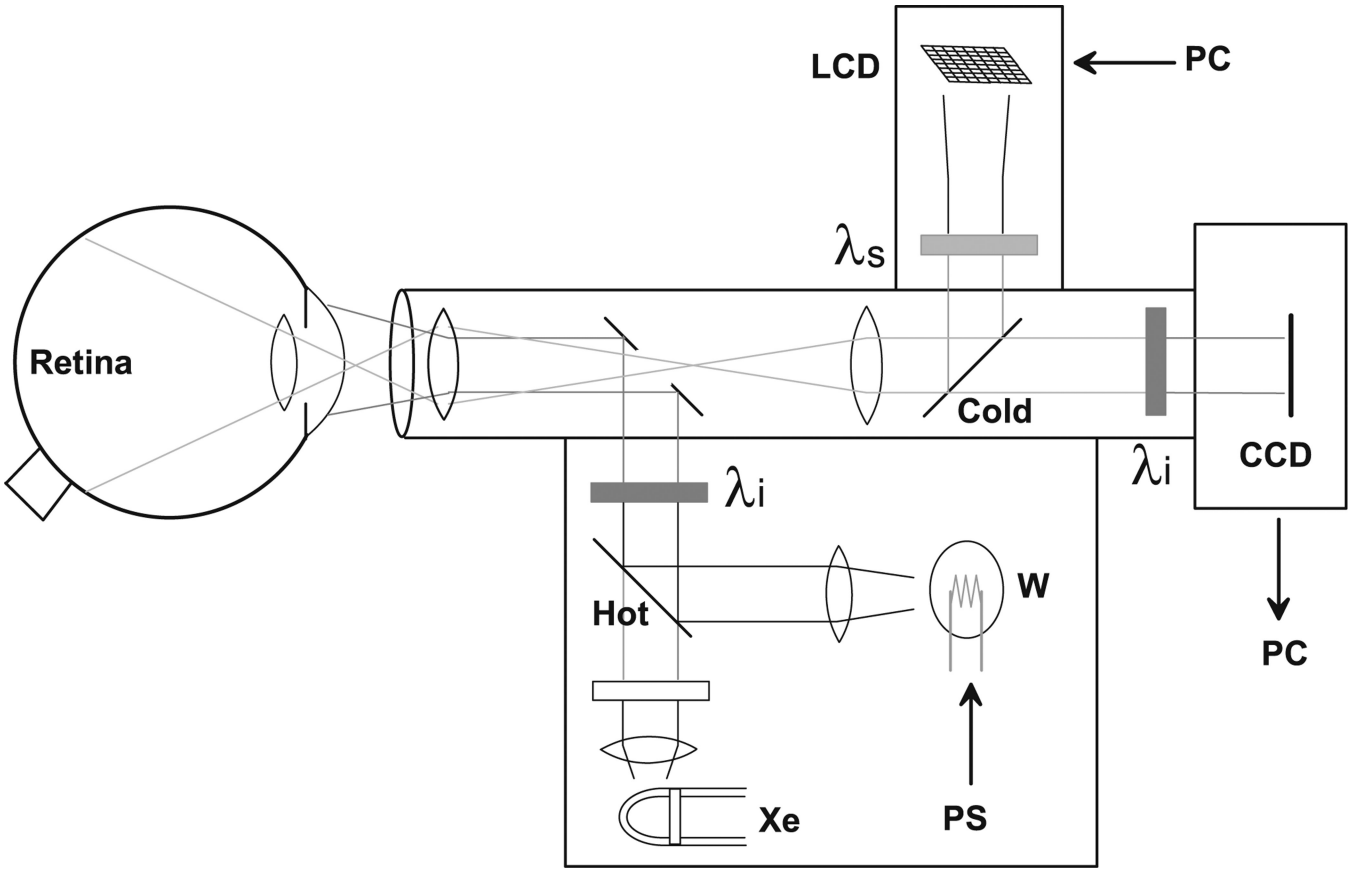

Figure 1.

Schematic diagram of a retinal optical imaging camera, based on a modified Topcon fundus camera. The retina is illuminated with near infrared (NIR) light (λi, 700–900 nm; typical, 750 nm) generated by the built-in tungsten lamp (*W*). The reflected NIR light is filtered to block any out-of-band light before being collected by the CCD camera. Visible patterned stimuli are generated by a small LCD module, filtered (λs, typically 540 nm green), and reflected into the light path projected onto the retina via a dichroic (cold) mirror. *PS*, power supply; *PC*, personal computer; *Xe*, Xenon flashlamp.

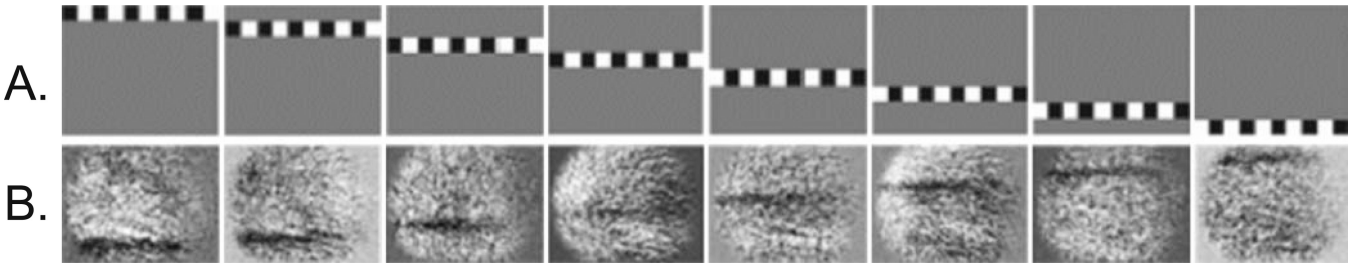

Figure 2.

A, B. Imaged retinal responses to a series of horizontal bar stimuli. **A** Series of horizontal counter-flickering checkerboard bar stimuli individually positioned to span the imaged portion of retina (−40°). **B** Optically imaged response to stimuli in **A**, imaged at 750 nm and analyzed by subtraction and division with the prestimulus baseline images (dR/R). Owing to the optics of the eye, the position of the activated region of the retina shifts from bottom to top as the position of the stimulus is shifted from top to bottom.

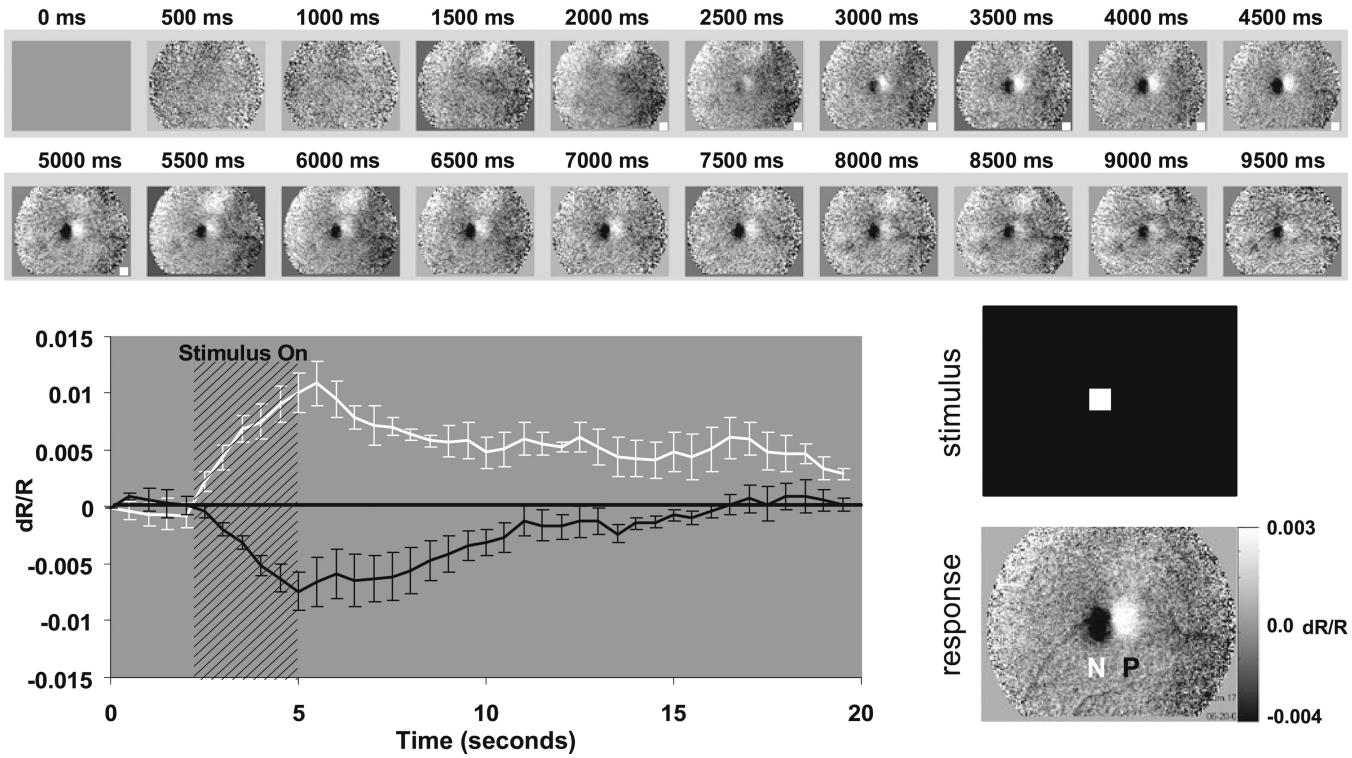

Figure 3.

Development sequence of the imaged signal. The measured intrinsic signals have a slow, monophasic rise time. Each frame shows the difference as the signal develops over time. Between 0 and 2000 ms, when no stimulus is presented, there is little change from baseline (middle-gray levels represent zero). Both positive (*white plotted line*) and negative (*black plotted line*) signals appear within 500 ms of stimulus onset and continue to grow in strength for the duration of the stimulus (3 s). Signals grow in magnitude, yet remain spatially coupled to the region of retinal stimulation. When the stimulus is turned off at 5000 ms, both signals remain, indicating that neither is an artifact of the stimulus energy. Signals have a slow decay back to baseline values. The time course of the regions of interest (ROIs) placed over the negative (*N*) and positive (*P*) signals can be seen below, showing that the negative and positive signals have matching time courses, suggesting a common or linked underlying mechanism.

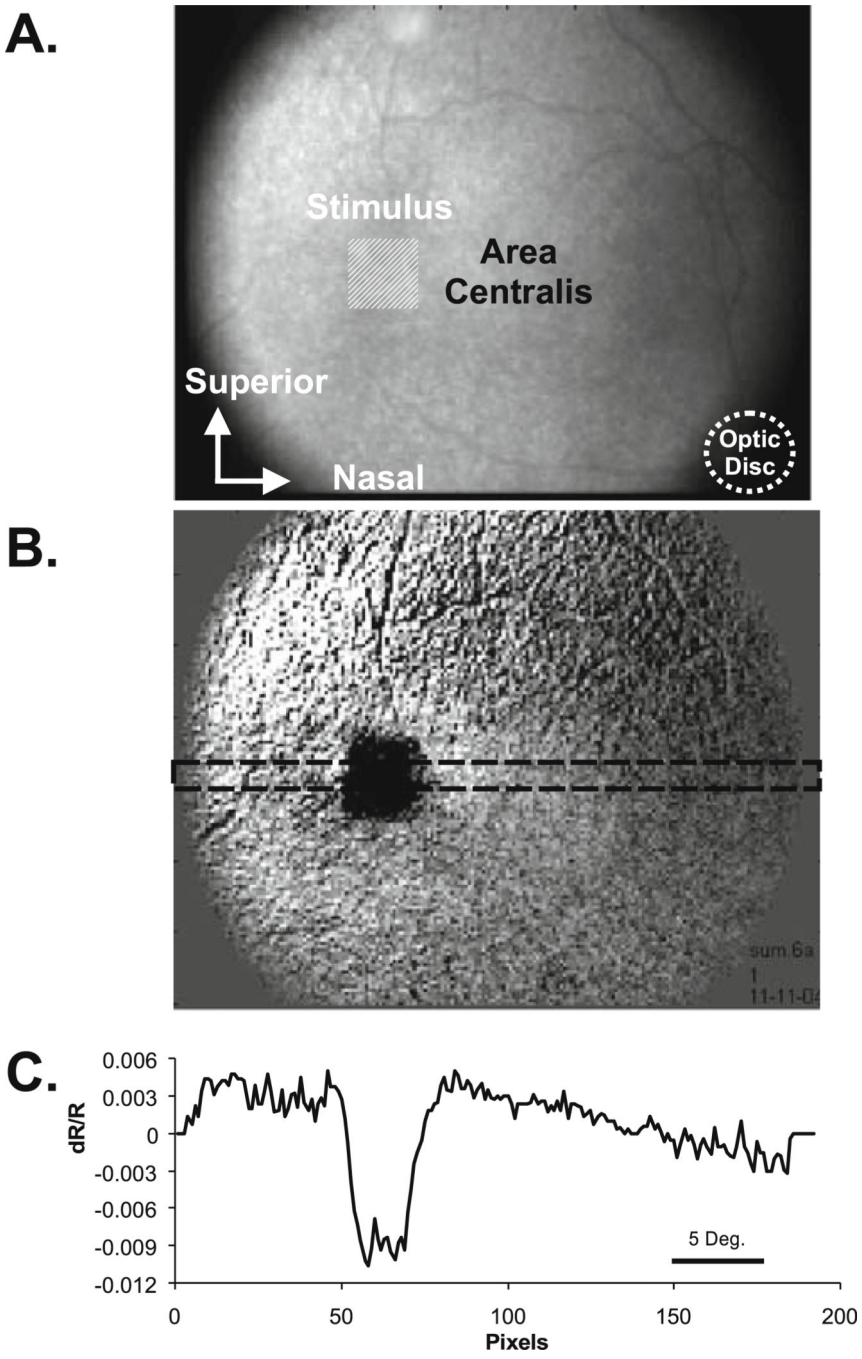

Figure 4.

A–C. Intrinsic signals demonstrate tight colocalization with the stimulated region of retina and a narrow line spread function. **A** A raw NIR reflectance image of the cat retina (right eye). The imaged area represents a 35° field of view. The optic disc is highlighted in the lower left corner. The superior and inferior vascular arcades emanate from the optic disc and can be seen in the inferior and superior regions of the image. The area centralis lies approximately 13° from the optic disc. The stimulus placement is represented by a *square, light-shaded* region. **B** A difference image reveals the spot activation in the NIR image. The

tight spatial coupling of the square spot stimulus can be seen. **C** A line profile of the reflectance signal is plotted. The data are the average values from the rectangular strip in **B** above. The sharp borders of the signal can be clearly seen against the background reflectance. This figure demonstrates a spatial resolution as sharp as 80 μm, corresponding to roughly 22 minutes of arc.

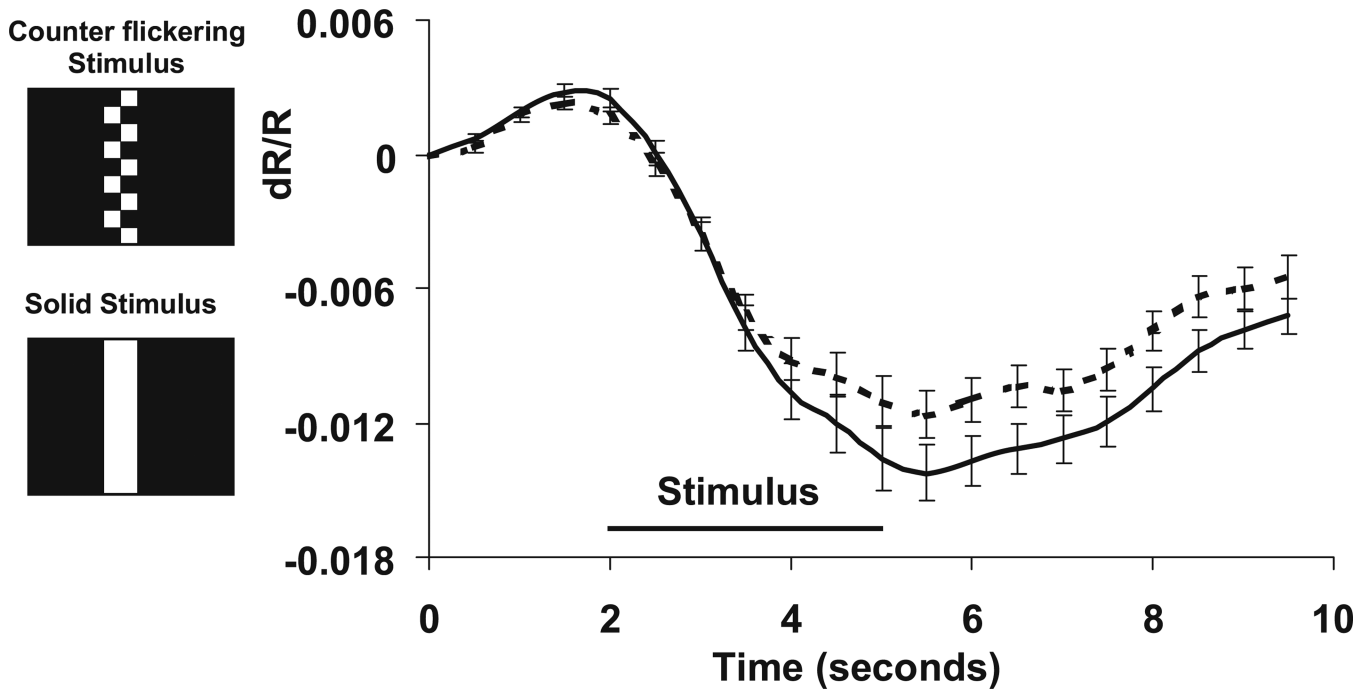

Figure 5.

Solid versus counter-flickering stimulus/response. Solid stimuli yielded signals of greater magnitude than counter-flickering stimuli. Negative intrinsic signals were measured at several ROIs. The averaged time course was 20 trials for each stimulus condition: counter flickering and solid. Solid stimuli (*solid plotted line*) consistently yielded signals greater than counter-flickering stimuli (*dashed plotted line*). This finding is inconsistent with a dominant signal source from the ganglion cell layer, which exhibits center-surround receptive fields that are spatially and temporally tuned. Error bars signify ± 1 SEM.

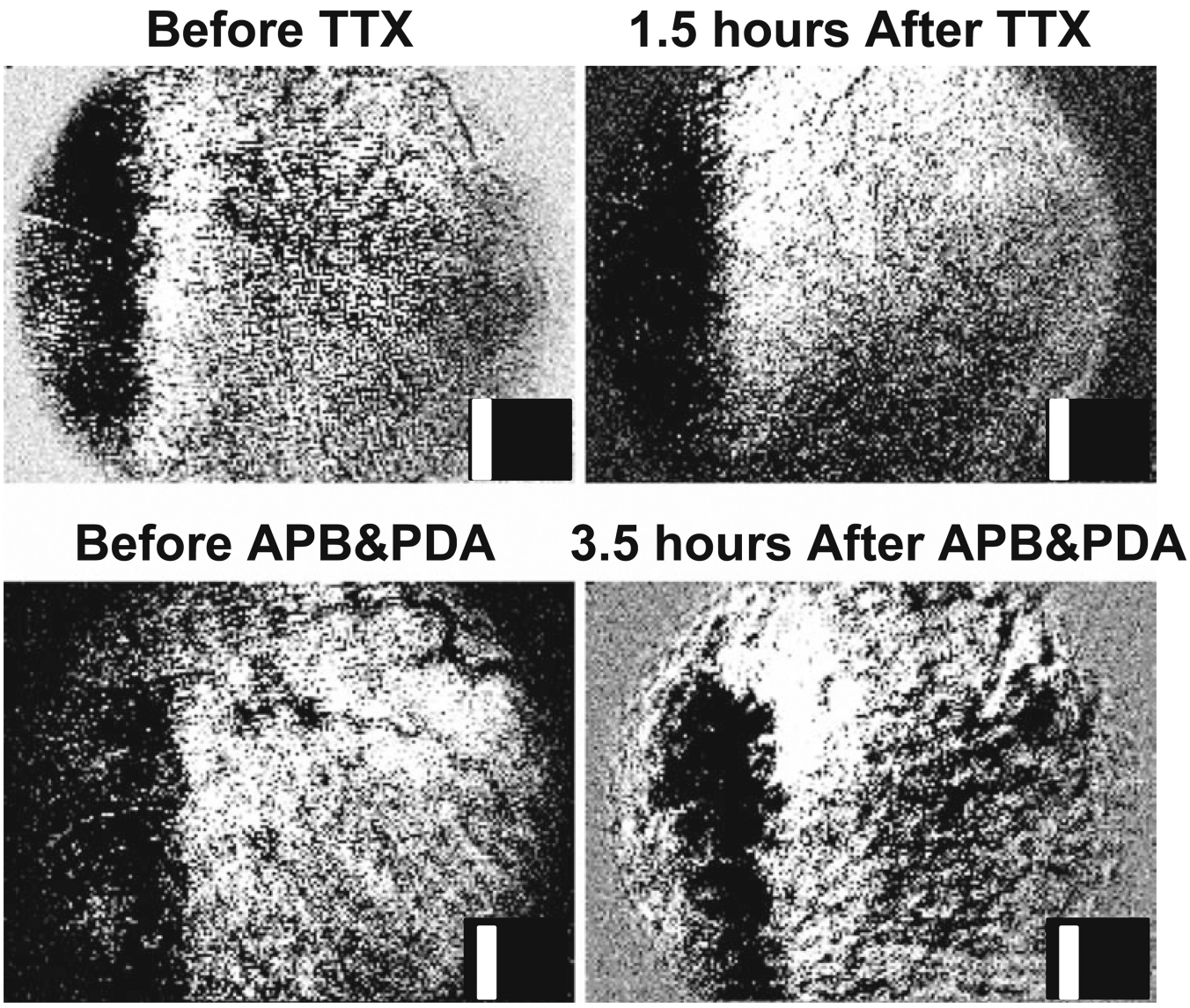

Figure 6.

Tetrodotoxin (*TTX*) and 2-amino-4-phosphonobutyric acid (*APB*) + cis-2,3-piperidinedicarboxylic acid (*PDA*) injections. Intrinsic signals remain after intravitreal injections of TTX or APB+PDA. *Top* The retina's response to a vertical bar before and 1.5 h after intravitreal injection of TTX (*inset*, example stimulus). Signals persist despite functional suppression of the ganglion cell layer [confirmed by an attenuated patterned electroretinogram (pERG) and the absence of consensual pupillary light reflex]. *Bottom* Intrinsic signals before and 3.5 h after a combined injection of APB and PDA. Signals remain colocalized with the stimulated region of retina after injection. Strong attenuation of the ON and OFF components of the long-pulse ERG confirm successful drug action at the photoreceptor–bipolar cell synapse.

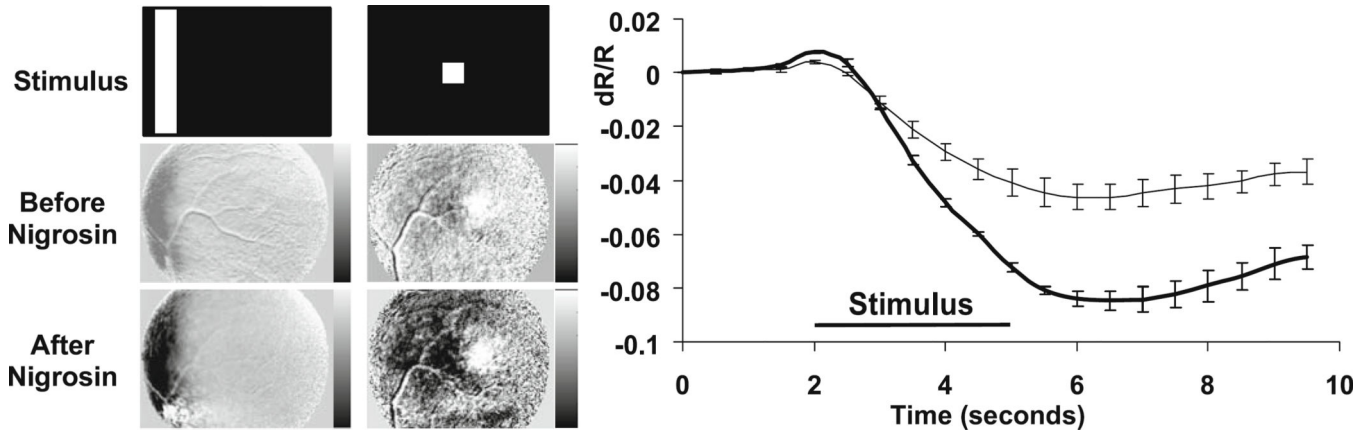

Figure 7.

Nigrosin circulatory contrast agent. Intrinsic signals increase in strength after systemic injection of nigrosin. The retina was imaged with 700-nm light before and after a single 34 mg/kg bolus of nigrosin. *Left* The grayscale maps show the retinal response for two stimulus conditions (*vertical bar* and *spot*). Middle images show the retina before nigrosin, and bottom images show signals at least 60 min after nigrosin. Images have been normalized to the postinjection value for that condition (bar condition grayscale range = 0.01 to −0.05 dR/R; spot condition grayscale range = 0.001 to −0.005 dR/R). Signal magnitudes are considerably larger after nigrosin injection. *Right* The time course of signals from ROIs overlying stimulated retinal sites quantified before (——) and after the injection (**—**). Intrinsic signals nearly doubled in magnitude for the 700-nm illumination condition. Other wavelengths showed more moderate but measurable signal increases (data not shown).

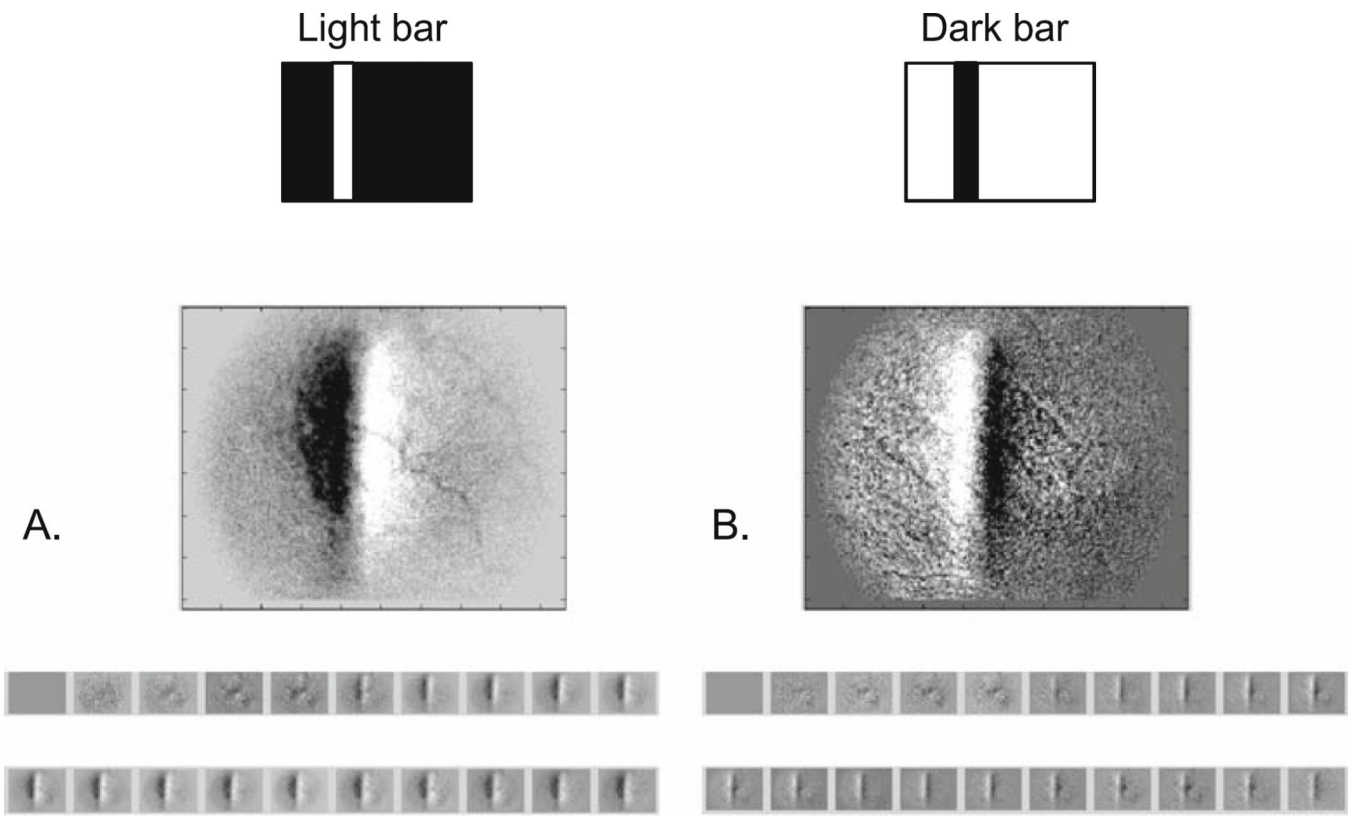

Figure 8.

A, B. Retinal signal signs invert with negative contrast stimuli. **A** The standard positive contrast stimulus (green bar on dark background) and retinal response (negative signal underlying the stimulated retina, positive signal nasal to the negative signal). **B** Negative contrast stimulus (dark bar on green background) and inverted retinal response (positive signal underlying stimulated retina and negative signal nasally adjacent to the positive signal). *Top* Stimulus configuration; *middle* imaged retinal response analyzed for dR/R; *bottom* temporal sequence of response images at a 2-Hz sample rate, showing signal development.

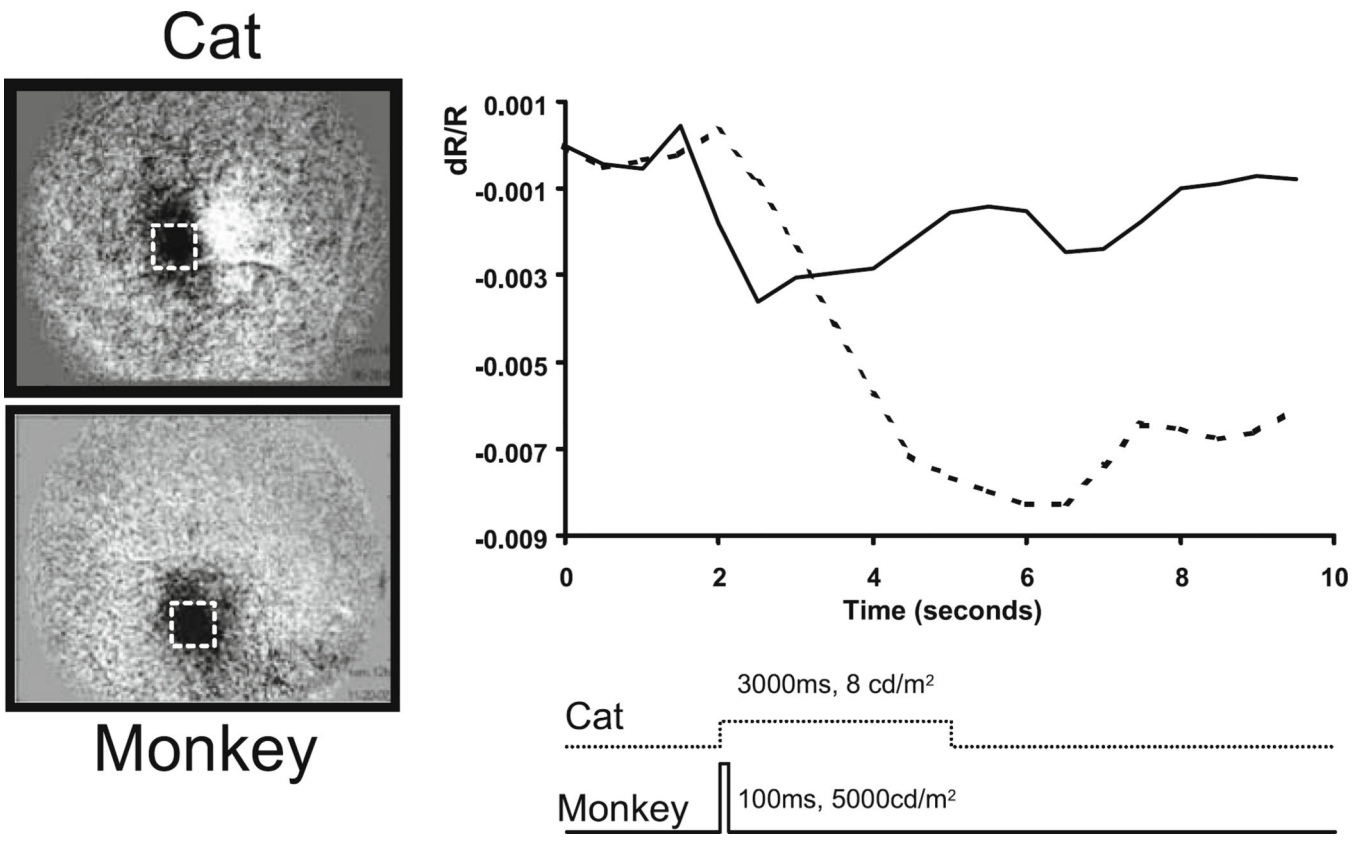

Figure 9.

Comparison of cat and monkey retinas. Intrinsic signals were observed in both species. *Left* A spot stimulus of 2–3° produced a negative signal underlying the stimulated region of retina in both species. *Right* Plotted time course of cat (------) and macaque monkey (——) signals. The macaque retina required very bright stimuli (5000 cd/m^2, approximately 1000-fold over the cat retina) in order to produce a comparable response. A mesopic stimulus of 8 cd/m^2 presented for 3 s yielded a high signal-tonoise response in the cat. A 100-ms pulse of light was used, which produced robust signals in the macaque retina.